Title
Crystallographic characterization of (C5H4SiMe3)3U(BH4)

Journal
Acta Crystallographica Section E: Crystallographic Communications, 77(Pt 4)

ISSN
2056-9890

Authors
Windorff, Cory J
Cross, Justin N
Scott, Brian L
et al.

Publication Date
2021-04-01

DOI
10.1107/s2056989021002425

Acta Cryst E CRYSTALLOGRAPHIC COMMUNICATIONS

ISSN 2056-9890

Crystallographic characterization of $(C_5H_4SiMe_3)_3U(BH_4)$

Cory J. Windorff,[a,b]‡ Justin N. Cross,[a] Brian L. Scott,[a] Stosh A. Kozimor[a]* and William J. Evans[b]*

[a]Los Alamos National Laboratory, Los Alamos, New Mexico 87544, USA, and [b]Department of Chemistry, University of California, Irvine, California 92697, USA. *Correspondence e-mail: stosh@lanl.gov, wevans@uci.edu

Received 6 January 2021
Accepted 3 March 2021

Edited by M. Zeller, Purdue University, USA

‡ Present address: New Mexico State University, Department of Chemistry and Biochemistry, Las Cruces, NM 88003, USA.

Keywords: crystal structure; uranium; borohydride; cyclopentadienyl compounds.

CCDC reference: 2067867

Supporting information: this article has supporting information at journals.iucr.org/e

New syntheses have been developed for the synthesis of (borohydrido-κ^3H)tris[η^5-(trimethylsilyl)cyclopentadienyl]uranium(IV), $[U(BH_4)(C_8H_{13}Si)_3]$ or $Cp'_3U(BH_4)$ ($Cp' = C_5H_4SiMe_3$) and its structure has been determined by single-crystal X-ray crystallography. This compound crystallized in the space group $P\overline{1}$ and the structure features three η^5-coordinated Cp′ rings and a κ^3-coordinated $(BH_4)^-$ ligand.

1. Chemical context

Actinide borohydrides have been of interest since the 1940s, owing to their potential volatility and applied use in vapor deposition technologies for the production of thin films (Hoekstra & Katz, 1949; Daly & Girolami, 2010). Uranium borohydride compounds are structurally interesting because the $(BH_4)^-$ ligand can coordinate large electropositive cations (such as uranium) in several modes. For example, κ^1, κ^2, and κ^3 U–(BH_4) binding has previously been reported (Ephritikhine, 1997). Borohydrides can also achieve high coordination numbers with uranium, *e.g.* the oligomeric 14-coordinate $U(BH_4)_4$ (Bernstein *et al.*, 1972). Although several cyclopentadienyl uranium borohydrides have been crystallographically characterized (Ephritikhine, 1997), the structure of $Cp'_3U(BH_4)$ ($Cp' = C_5H_4SiMe_3$), made in 1992 (Berthet & Ephritikhine, 1992), has not been reported. Our interest in Cp′ uranium chemistry (MacDonald *et al.*, 2013; Windorff *et al.*, 2017) prompted us to determine the coordination mode of $(BH_4)^-$ within the tris-cyclopentadienyl uranium platform using single-crystal X-ray diffraction. Toward this end, we developed new synthetic routes to the $Cp'_3U(BH_4)$ compound.

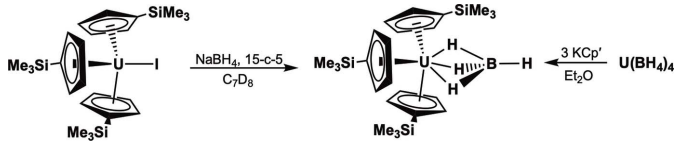

The $Cp'_3U(BH_4)$ compound was originally synthesized by reacting Cp'_3UH with H_3B-PPh_3 (Berthet & Ephritikhine, 1992). Our attempts to repeat this procedure in toluene and diethyl ether solvents were unsuccessful, potentially because we were uncertain about the details of the reaction. However, we were successful in synthesizing $Cp'_3U(BH_4)$ from Cp'_3UH with H_3B-PPh_3 in hot THF solvent. We also observed $Cp'_3U(BH_4)$ could be prepared in high yield (96%) by reacting

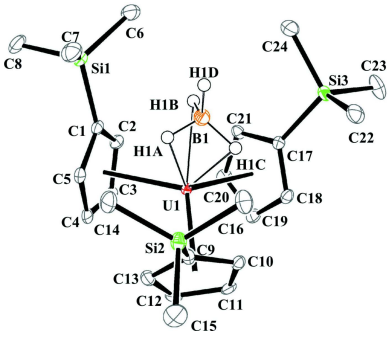

Table 1
A comparison of structural parameters (Å, °) in $Cp'_3U(BH_4)$ and other Cp'_3UX {X = Cl^-, I^-, $[Si(SiMe_3)_3]^-$} complexes.

cent = $C_5H_4SiMe_3$ centroid.

	$Cp'_3U(BH_4)$	Cp'_3UCl[a] (Windorff *et al.*, 2017)	Cp'_3UI (Windorff *et al.*, 2017)	$Cp'_3U(\eta^1\text{-}CH{=}CH_2)$ (Schock *et al.*, 1988)	$Cp'_3U[Si(SiMe_3)_3]$ (Réant *et al.*, 2020)
U—(cent)	2.458, 2.490, 2.500	2.473	2.475, 2.478, 2.480	2.481, 2.483, 2.489	2.472, 2.478, 2.485
(cent)—U—X	104.13, 104.14, 104.83	100.00	97.9, 101.2, 101.6	95.1 100.0 100.2	96.04, 96.30, 97.65
(cent)—U—(cent)	113.28, 114.26, 114.26	117.00	116.1, 116.4, 118.3	116.4, 117.2, 120.0	118.28, 118.88, 119.08

Note: (*a*) The asymmetric unit contains one Cp′ ring, one-third of a chloride atom, and one-third of a uranium atom.

Cp'_3UI with $NaBH_4$ in the presence of 15-crown-5. When this reaction was carried out in toluene at room temperature, the I^- ligand was substituted by the $(BH_4)^-$ anion. Another method we developed for synthesizing $Cp'_3U(BH_4)$ involved reacting $U(BH_4)_4$ with KCp′ (3 equiv.) in diethyl ether. This reaction, where $(BH_4)^-$ was substituted by $(Cp')^-$, also proceeded in high yield (89%). X-ray quality crystals of $Cp'_3U(BH_4)$ formed at 253 K overnight from diethyl ether solutions.

Of our two synthetic routes, we preferred making $Cp'_3U(BH_4)$ from Cp'_3UI over $U(BH_4)_4$ because the $U(BH_4)_4$ starting material was more challenging to isolate in a chemically pure form. Another interesting comparison between the two synthetic methods involved the substitution chemistry. The $(Cp')^-$ anion displaced $(BH_4)^-$ from $U(BH_4)_4$ and $(BH_4)^-$ displaced I^- in Cp'_3UI. Hence, we qualitatively concluded that the stability of the U—X bond for molecular compounds dissolved in organic solvents was largest for $(Cp')^-$, intermediate for $(BH_4)^-$, and lowest for I^-. The generality of this conclusion is limited, and we acknowledge the solubility of the other reaction products (such as NaI) might significantly influence the substitution chemistry on uranium.

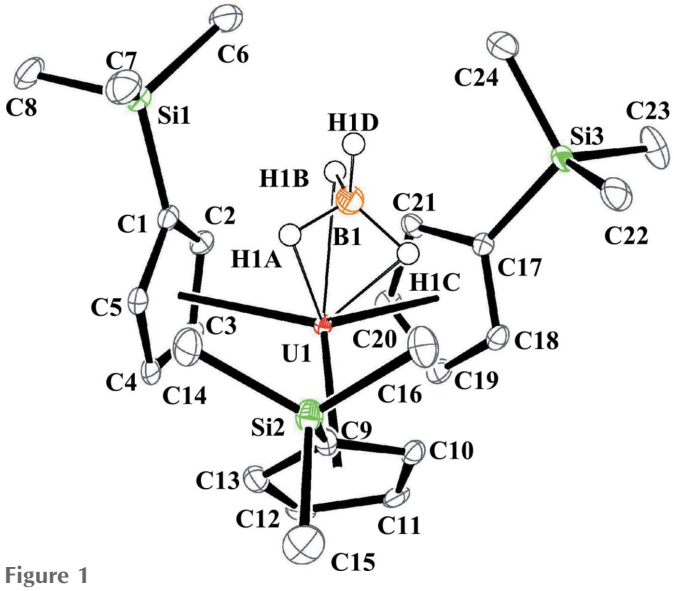

Figure 1
Structure of $Cp'_3U(BH_4)$ with atomic displacement parameters drawn at the 50% probability level. Boron-bound hydrogen atoms are represented as isotropic circles. All carbon-bound hydrogen atoms are omitted. Selected structural metrics, U—(Cp′ centroid) average 2.48 (2) Å, U—H average 2.35 (1) Å, (Cp′ centroid)—U—(Cp′ centroid) average 113.9 (6)°, (Cp′ centroid)—U—B average 104.4 (4)°, and terminal B—H distance of 1.11 (5) Å.

2. Structural commentary

Single crystal X-ray data from $Cp'_3U(BH_4)$ were refined in the triclinic $P\overline{1}$ space group with one crystallographically unique molecule in the unit cell, see Fig. 1. The data are of high quality, and electron-density difference peaks consistent with the location and geometry of bridging hydrides were located from a difference-Fourier map with U—H distances of 2.35 (5), 2.35 (5), and 2.36 (5) Å. Although the uncertainty associated with the U—H bonds is relatively high, they are consistent with previously reported bond lengths for actinide(IV) hydride interactions (Ephritikhine, 1997; Daly *et al.*, 2010). Significantly lower uncertainty is associated with the U—B distance at 2.568 (4) Å, which is similar to two of the three U—B distances in $[U(BH_4)_3(DME)]_2(\mu\text{-}O)$ (DME = 1,2-dimethoxyethane), 2.574 (6), 2.584 (6), and 2.635 (7) Å (Daly *et al.*, 2012). The U—B distance in $(C_5H_5)_3U(BH_4)$ was reported to be 2.48 Å (Zanella *et al.*, 1988), although disorder in that structure prevented a full solution from being obtained. Theoretical calculations on $(C_5H_5)_3U(BH_4)$ in the gas phase and in solution predicted U—B distances of 2.533 and 2.557 Å (Elkechai *et al.*, 2009), which are also consistent with our data. Other $(C_5R_5)_2U(BH_4)_2$ structures showed similar U—B distances of 2.56 (1) Å for $[C_5H_3(SiMe_3)_2]_2U(BH_4)_2$ (Blake *et al.*, 1995), 2.58 (3) Å in $(C_5Me_5)_2U(BH_4)_2$ (Gradoz *et al.*, 1994, Marsh *et al.*, 2002), and 2.553 (1) Å in $(PC_4Me_4)_2U(BH_4)_2$ (Baudry *et al.*, 1990).

The uranium–(Cp′ centroid) distances in $Cp'_3U(BH_4)$ range from 2.458–2.500 Å and average 2.48 (2) Å (uncertainty reported as the standard deviation from the mean at 1σ). These uranium–(Cp′ centroid) distances compare well with the 2.473 Å analogous metric in Cp'_3UCl (Windorff *et al.*, 2017) and other Cp'_3UX structures (see Table 1) with average U–(Cp′ centroid) distances of 2.478 (3) Å in Cp'_3UI (Windorff *et al.*, 2017), 2.484 (4) Å in $Cp'_3U(\eta^1\text{-}CH{=}CH_2)$ (Schock *et al.*, 1988) and 2.478 (7) Å in $Cp'_3U[Si(SiMe_3)_3]$ (Réant *et al.*, 2020). The 113.9 (6)° average of (Cp′ centroid)—U—(Cp′ centroid) angles in $Cp'_3U(BH_4)$ is more acute than the 117.0° angle in Cp'_3UCl and other Cp'_3UX structures, where the average (Cp′ centroid)—U—(Cp′ centroid) angles were reported as 117 (1)° in Cp'_3UI, 112 (2)° in $Cp'_3U(\eta^1$-

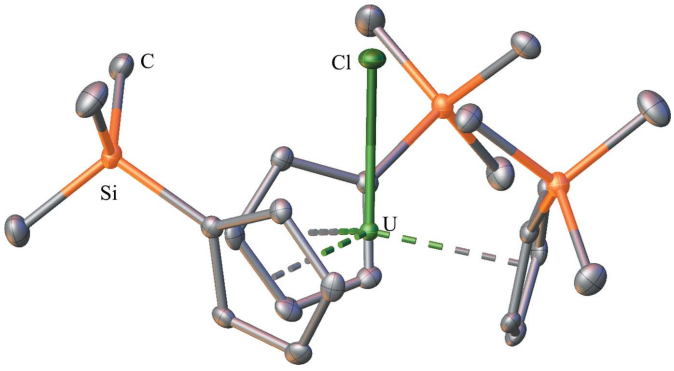

Figure 2
Structure of Cp'_3UCl with atomic displacement parameters drawn at the 50% probability level, as reproduced from the published CIF (Windorff *et al.*, 2017); the isomorphous thorium complex, Cp'_3ThCl, is also known (Réant *et al.*, 2020). Hydrogen atoms are omitted for clarity.

CH═CH_2), and 118.7 (4)° in $Cp'_3U[Si(SiMe_3)_3]$. The more acute (Cp′ centroid)—U—(Cp′ centroid) angles are complemented by a more obtuse average (Cp′ centroid)—U—B angle of 104.4 (4)° in $Cp'_3U(BH_4)$, likely due to the close proximity

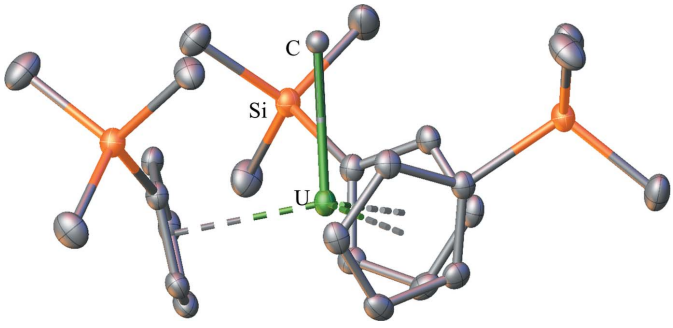

Figure 3
Structure of Cp'_3UCH_3/Cl with only the $(CH_3)^-$ ligand shown, with atomic displacement parameters drawn at the 50% probability level, except the $-CH_3$ unit, which has been plotted as an isotropic sphere, as reproduced from the published CIF (Windorff *et al.*, 2017), see the manuscript for further details. Hydrogen atoms are omitted for clarity.

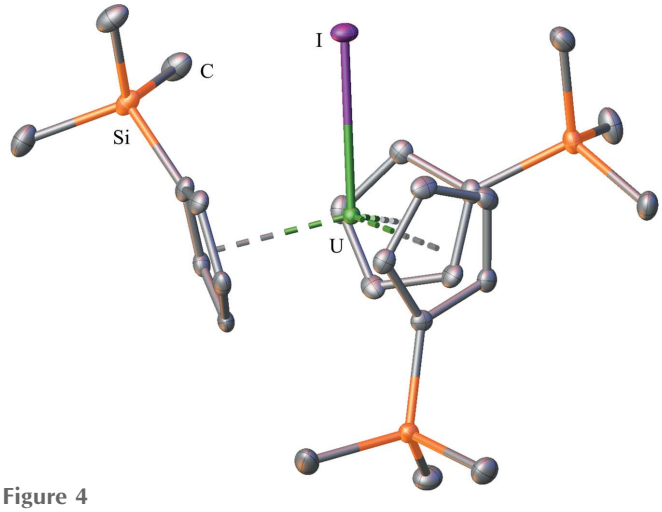

Figure 4
Structure of Cp'_3UI with atomic displacement parameters drawn at the 50% probability level, as reproduced from the published CIF (Windorff *et al.*, 2017). Hydrogen atoms are omitted for clarity.

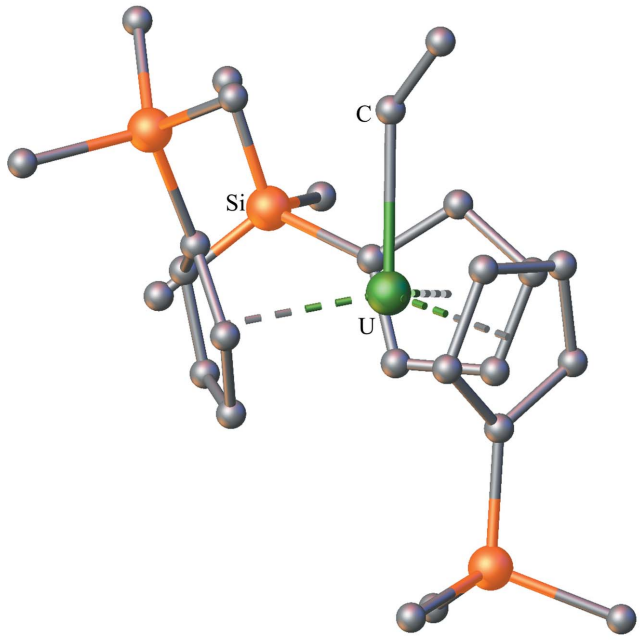

Figure 5
Structure of $Cp'_3U(\eta^1\text{-}CH{=}CH_2)$ with atomic displacement parameters drawn as isotropic spheres, as reproduced from the CIF (Schock *et al.*, 1988). Hydrogen atoms are omitted for clarity.

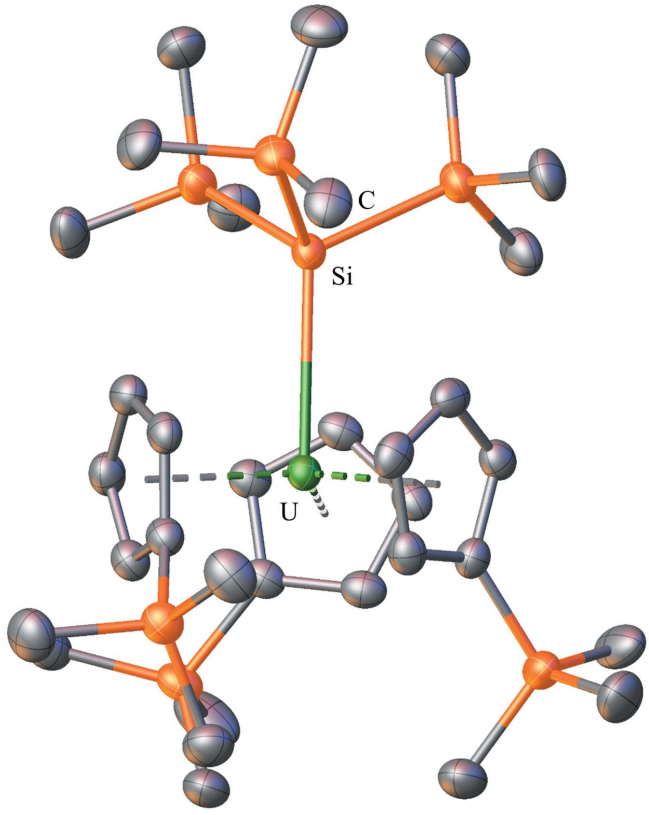

Figure 6
Structure of $Cp'_3U[Si(SiMe_3)_3]$ with atomic displacement parameters drawn at the 50% probability level, as reproduced from the published CIF (Réant *et al.*, 2020); the isomorphous thorium complex, $Cp'_3Th[Si(SiMe_3)_3]$, is also known (Réant *et al.*, 2020). Hydrogen atoms are omitted for clarity.

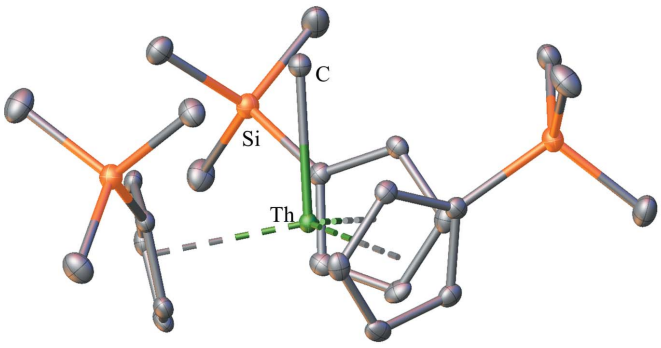

Figure 7
Structure of Cp'_3ThCH_3 with atomic displacement parameters drawn at the 50% probability level, as reproduced from the published CIF (Wedal *et al.*, 2019). Hydrogen atoms are omitted for clarity.

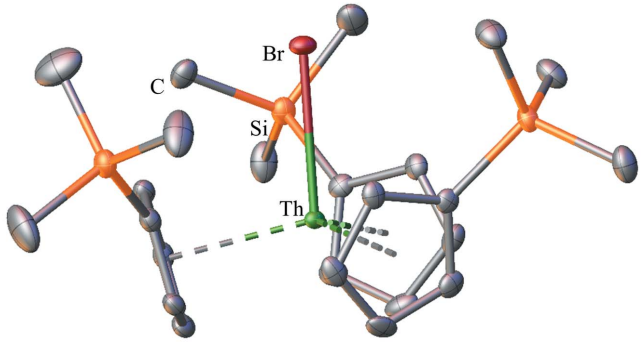

Figure 8
Structure of Cp'_3ThBr with atomic displacement parameters drawn at the 50% probability level, as reproduced from the published CIF in the $P\overline{3}$ space group (Windorff *et al.*, 2017); there is a second report of the same molecule in the $P2_1/c$ space group, featuring the same ligand orientation (Wedal *et al.*, 2019). Hydrogen atoms are omitted for clarity.

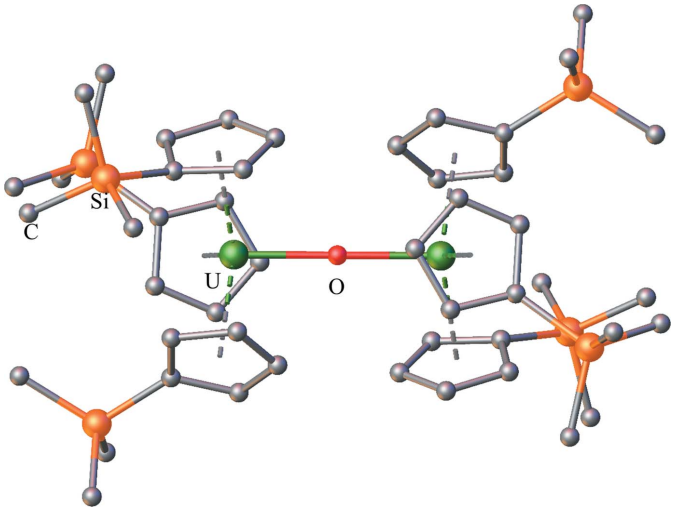

Figure 9
Structure of $(Cp'_3U)_2(\mu\text{-O})$ with atomic displacement parameters drawn as isotropic spheres, as reproduced from the CIF (Berthet *et al.*, 1991); the isomorphous thorium complex, $(Cp'_3Th)_2(\mu\text{-O})$, is also known (Wedal *et al.*, 2019). Hydrogen atoms are omitted for clarity.

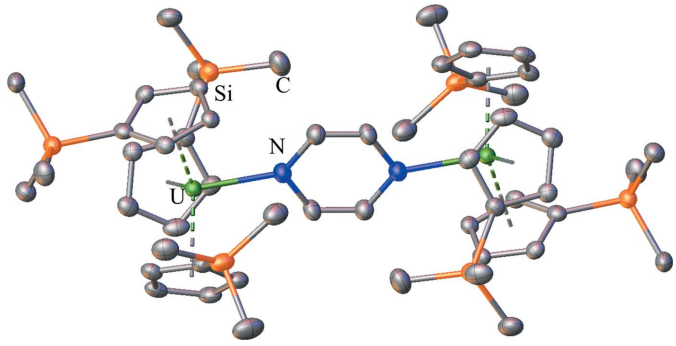

Figure 10
Structure of $(Cp'_3U)_2[\mu\text{-}(N_2C_4H_4)]$ with atomic displacement parameters drawn at the 50% probability level, as reproduced from the published CIF (Mehdoui *et al.*, 2004). Hydrogen atoms are omitted for clarity.

of the $(BH_4)^{1-}$ ligand compared with (Cp′ centroid)—U—*X* angles of 100.0° in Cp'_3UCl, 100 (2)° in Cp'_3UI, 98 (3)° in $Cp'_3U(\eta^1\text{-}CH{=}CH_2)$, and 96.7 (9)° in $Cp'_3U[Si(SiMe_3)_3]$, see Table 1.

An unusual feature of the $Cp'_3U(BH_4)$ structure is that all three of the trimethylsilyl groups are oriented in a single direction towards the $(BH_4)^-$ unit. This orientation has not been observed in other Cp'_3U(anion) and $Cp'_3U(\mu$-dianion)UCp'_3 structures, which are shown in Figs. 2–12. The closest comparison is with the Cp'_3UCl structure (Windorff *et al.*, 2017), where all three trimethylsilyl groups are oriented towards the Cl^- unit, but twisted down and away from the chloride towards the meridian. The Cp'_3UI (Windorff *et al.*, 2017) and $Cp'_3U(\eta^1\text{-}CH{=}CH_2)$ (Schock *et al.*, 1988) complexes have one trimethylsilyl group pointed away from the anionic ligand. The $Cp'_3U[Si(SiMe_3)_3]$ complex (Réant *et al.*, 2020) represents the opposite extreme where all of the

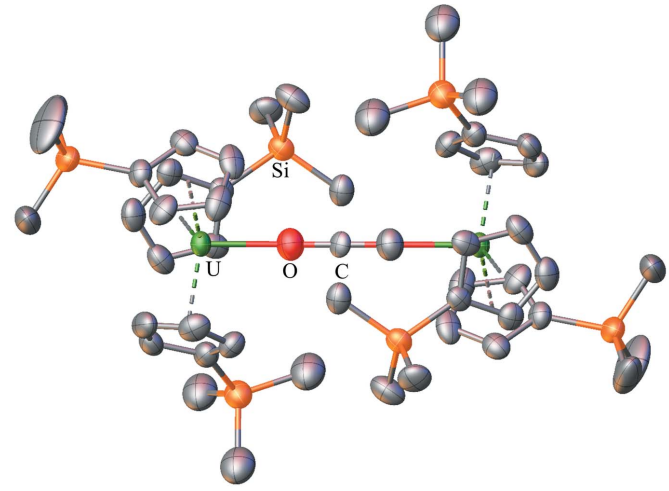

Figure 11
Structure of $(Cp'_3U)_2(\mu\text{-CCO})$ with atomic displacement parameters drawn at the 50% probability level and disorder in the $(\mu\text{-CCO})^{2-}$ unit displayed in one configuration, as reproduced from the published CIF (Tsoureas & Cloke, 2018). The molecule contains a plane of symmetry, and the unit cell contains two half molecules with the same orientation. For clarity, only one full molecular unit is depicted and hydrogen atoms are omitted for clarity.

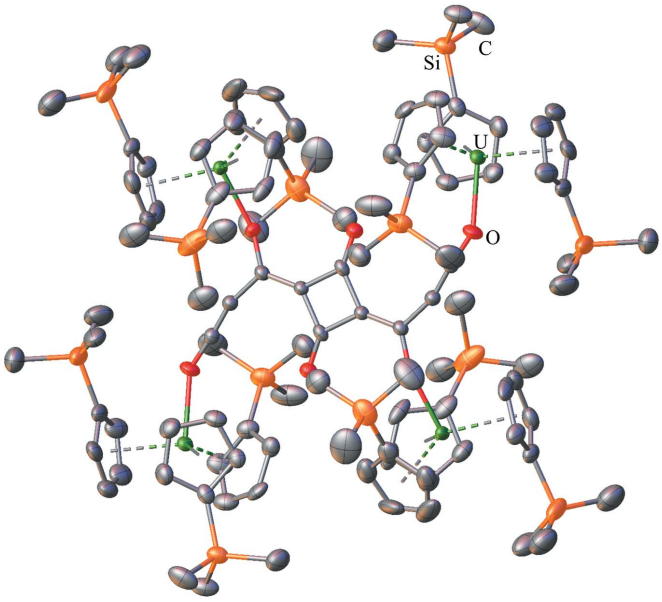

Figure 12
Structure of $(Cp'_3U)_4(\mu\text{-}L)$ where L = a complex organic structure containing a central cyclobutene-1,3-dione ring, with atomic displacement parameters drawn at the 50% probability level, as reproduced from the published CIF (Tsoureas & Cloke, 2018). Hydrogen atoms and disorder in the $-SiMe_3$ groups are omitted for clarity.

trimethylsilyl groups are oriented away from the $[Si(SiMe_3)_3]^{1-}$ unit. Since $Cp'_3U(BH_4)$ has the smallest mono-anion of the Cp'_3U(anion) complexes and the correspondingly smallest (Cp′ centroid)—U—(Cp′ centroid), and the largest (Cp′ centroid)—U—X angles, the orientation of the silyl groups could occur due to steric factors. However, it is also possible that some dispersion forces between the $(BH_4)^-$ and the trimethylsilyl groups could contribute to the orientation (Liptrot *et al.*, 2016). It is interesting to note that in the Cp'_3ThX series where X = Cl (Réant *et al.*, 2020), Br (Windorff *et al.*, 2017), and CH_3 (Wedal *et al.*, 2019), all three trimethylsilyl groups are oriented towards the anion, but twisted down and away from the anion towards the meridian as in Cp'_3UCl.

3. Supramolecular features

There are no major supramolecular features to report. The molecules pack in an alternating 180° rotation from one another within the unit cell and stack 'head to tail' between the unit cells.

4. Database survey

A search using the Cambridge Structural Database (Version 5.41, March 2020; Groom *et al.*, 2016) for borohydride structures containing η^5-aromatic five-membered rings bound to uranium showed two classes of complexes. There were the uranium(IV) piano-stool complexes: $(C_5H_5)U(BH_4)_3$ (DEKVEU and DEKVEU10; Baudry *et al.*, 1985, 1989); $(C_5Me_5)U(BH_4)(SPS^{Me})$ (JOJTIM; Arliguie *et al.*, 2008), where SPS^{Me} = PC_5H-3,5-Ph,-2,6-$(P(S)Ph_2)$-1-Me, a λ^4-phosphinine with two lateral phosphinosulfide groups, and the tetramethylphosphol (PC_4Me_4) compound $(PC_4Me_4)(C_8H_8)U(BH_4)(THF)$ (MOBVEE; Cendrowski-Guillaume *et al.*, 2002). There were also uranium(IV) metallocene structures, $(Ring)_2U(BH_4)_2$, where Ring = C_5H_5 (CPURBH; Zanella *et al.*, 1977), $C_5H_3(SiMe_3)_2$ (ZEYZOS; Blake *et al.*, 1995), C_5Me_5 (WIFFOG and WIFFOG01; Gradoz *et al.*, 1994; Marsh *et al.*, 2002), C_9H_7 (VASVUG, C_9H_7 = indenide; Rebizant *et al.*, 1989) and PC_4Me_4 (KIJBEK, PC_4Me_4 = tetramethylphosphol; Baudry *et al.*, 1990). The macrocyclic *trans*-calix[2]benzene[2]pyrrolide (L) complex $[LU(BH_4)][B(C_6F_5)_4]$ was also in the database (CUJMEB; Arnold *et al.*, 2015). This last compound features two η^5-bound $NC_4H_2R_2$ ligands. Also in the database were a few examples of uranium(III) borohydrides, such as the mono borohydride $[(PC_4Me_4)_2U(BH_4)]_2$ (YEZJES; Gradoz *et al.*, 1994) and the mixed oxidation state piano stool $[Na(THF)_6][(C_5Me_5)U(BH_4)_3]_2$ (VAXMUC; Ryan *et al.*, 1989)] complexes.

There are also three dimeric uranium(IV) complexes with Cp'^- ligands, all of the form $(Cp'_3U)_2(\mu\text{-}X)$ where $X = O^{2-}$ (SOSXON; Berthet *et al.*, 1991), $(pyrazine)^{2-}$, $(N_2C_4H_4)^{2-}$ (EYERIJ; Mehdoui *et al.*, 2004), and CCO^{2-} (PIKFAT; Tsoureas & Cloke, 2018). There is also the tetrametallic $(Cp'_3U)_4(\mu\text{-}L)$ (PIKDUL; Tsoureas & Cloke, 2018) where L is a complex organic structure containing a central cyclobutene-1,3-dione ring.

5. Spectroscopic Features

The fully defined $Cp'_3U(BH_4)$ compound was also characterized by ^1H, $^{11}B\{^1H\}$, $^{13}C\{^1H\}$, and $^{29}Si\{^1H\}$ multi-nuclear NMR spectroscopy. It was of particular interest to examine the $^{29}Si\{^1H\}$ spectrum for comparison with previous studies of silicon-containing paramagnetic uranium complexes (Windorff & Evans, 2014). The ^1H NMR spectrum in C_7D_8 was in good agreement with the literature (Berthet & Ephritikhine, 1992). $^{11}B\{^1H\}$, $^{13}C\{^1H\}$, and $^{29}Si\{^1H\}$ spectra were also obtained in both C_7D_8 and C_6D_6, as well as different field strengths, 500 *vs* 600 MHz for ^1H, to see if any significant solvent or field effects were present. Since the spectra were not dependent on solvent or field strength, only the spectra obtained in C_6D_6 in a 600 MHz field will be discussed here. See Section 6 for full details.

In general, the resonances attributable to the Cp'^- ligands are sharp ($\nu_{1/2}$ < 50 Hz) and paramagnetically shifted over a range of δ 9.6 to −22.6 ppm, in the ^1H NMR spectrum, and a $^{29}Si\{^1H\}$ resonance at δ −57.4 ppm was observed, typical of other tetravalent uranium complexes (Windorff & Evans, 2014). The resonances attributable to the $(BH_4)^-$ unit showed considerably more shifting and broadening, resonating at δ −59.5 ($\nu_{1/2}$ = 300 Hz) and 79.6 ($\nu_{1/2}$ = 240 Hz) in the ^1H and $^{11}B\{^1H\}$ spectra, respectively. Since the $(BH_4)^-$ ligand exhibited a single ^1H NMR resonance whereas two distinct hydride environments are present in the solid state, it appears that the complex is fluxional in solution. This is in line with previous studies (Ephritikhine, 1997).

6. Synthesis and crystallization

6.1. General considerations

All manipulations and syntheses described below were conducted with the rigorous exclusion of air and water using glovebox techniques under an argon atmosphere. Solvents (THF, Et_2O, toluene, hexane, and pentane) were sparged with UHP argon (Praxair) and dried by passage through columns containing a copper(II) oxide oxygen scavenger (Q-5) and molecular sieves prior to use or stirred over sodium benzophenone ketyl, briefly exposed to vacuum several times to degas and distilled under vacuum. All ethereal solvents were stored over activated 4 Å molecular sieves. Deuterated solvents (Cambridge Isotopes) used for nuclear magnetic resonance (NMR) spectroscopy were dried over sodium benzophenone ketyl, degassed by three freeze-pump-thaw cycles, and distilled under vacuum before use. The ^{1}H, ^{11}B{^{1}H}, ^{13}C{^{1}H} and ^{29}Si{^{1}H} NMR spectra were recorded on a GN 500, Cryo 500 or Bruker Avance 600 spectrometer operating at 500.2 MHz, 160.1 MHz, 125.8 MHz, and 99.1 MHz for the 500 MHz spectrometers, respectively, and 600.1 MHz, 192.6 MHz, 150.9 MHz and 119.2 MHz for the 600 MHz spectrometer, respectively, at 298 K unless otherwise stated. The ^{1}H and ^{13}C{^{1}H} NMR spectra were referenced internally to solvent resonances, ^{11}B and ^{29}Si{^{1}H} NMR spectra were referenced externally to $BF_3(Et_2O)$ and $SiMe_4$, respectively, the ^{29}Si{^{1}H} spectra were acquired using the INEPT pulse sequence. The 15-crown-5 (Aldrich) reagent was dried over activated molecular sieves and degassed by three freeze–pump–thaw cycles before use. The $NaBH_4$ (Aldrich) reagent was placed under vacuum (10^{-3} Torr) for 12 h before use. The following compounds were prepared following literature procedures: KCp′ (Peterson *et al.*, 2013), $U(BH_4)_4$ (Schlesinger & Brown, 1953), Cp′$_3$UI (Windorff *et al.*, 2017).

6.2. Cp′$_3$U(BH$_4$) from Cp′$_3$UI, NaBH$_4$ and 15-crown-5

Solid $NaBH_4$ (15 mg, 0.40 mmol) was added to a C_7D_8 (toluene-d_8, 0.6 mL) solution of Cp′$_3$UI (37 mg, 0.048 mmol) in a J-Young NMR tube, an excess of 15-crown-5 (1 drop) was added and the tube was sealed and removed from the glovebox and vortexed (30 s). The $NaBH_4$ was not fully soluble in C_7D_8 even in the presence of 15-crown-5. After 18 h, NMR spectroscopy showed complete conversion to Cp′$_3$U(BH$_4$). The sample was brought back into the glovebox and the volatiles were removed under reduced pressure. The product was then extracted into Et_2O, filtered away from white insoluble solids [presumably Na(15-crown-5)I and excess $NaBH_4$] and the volatiles were removed under reduced pressure to give Cp′$_3$U(BH$_4$) (30 mg, 96%) as a wine-red solid. ^{1}H NMR (C_7D_8, 500.2 MHz): δ 9.7 (*s*, $C_5H_4SiMe_3$, 6H), −2.1 (*s*, $C_5H_4Si\mathit{Me}_3$, 27H), −23.1 (*s*, $C_5\mathit{H}_4SiMe_3$, 6H), −59.8 (*s*, *br*, $\nu_{1/2}$ = 325 Hz, U−(BH_4), 4H); ^{11}B{^{1}H} NMR (C_7D_8, 160.1 MHz): δ 79.1 [*s*, *br*, $\nu_{1/2}$ = 230 Hz, U−(BH$_4$)]; ^{13}C{^{1}H} NMR (C_7D_8, 125.8 MHz): δ 233.1 ($\mathit{C}_5H_4SiMe_3$), 214.0 ($\mathit{C}_5H_4SiMe_3$), 185.6 ($\mathit{C}_5H_4SiMe_3$), 0.4 ($C_5H_4Si\mathit{Me}_3$); ^{29}Si{^{1}H} NMR (C_7D_8, 99.1 MHz, INEPT): δ −57.7 (*s*, $C_5H_4\mathit{Si}Me_3$); ^{1}H NMR (C_6D_6, 600.1 MHz): δ 9.6 (*s*, $C_5\mathit{H}_4SiMe_3$, 6H), −2.0 (*s*, $C_5H_4Si\mathit{Me}_3$, 27H), −22.6 (*s*, $C_5\mathit{H}_4SiMe_3$, 6H), −59.3 (*s*, *br*, $\nu_{1/2}$ = 300 Hz, U−(BH_4), 4H); ^{11}B{^{1}H} NMR (C_6D_6, 192.6 MHz): δ 79.6 [*s*, *br*, $\nu_{1/2}$ = 240 Hz, U-(BH$_4$)]; ^{13}C{^{1}H} NMR (C_6D_6, 150.9 MHz): δ 232.0 ($\mathit{C}_5H_4SiMe_3$), 214.2 ($\mathit{C}_5H_4SiMe_3$), 186.5 ($\mathit{C}_5H_4SiMe_3$), 0.6 ($C_5H_4Si\mathit{Me}_3$); ^{29}Si{^{1}H} NMR (C_6D_6, 119.2 MHz, INEPT): δ −57.4 (*s*, $C_5H_4\mathit{Si}Me_3$).

6.3. Cp′$_3$U(BH$_4$) from U(BH$_4$)$_4$ and KCp′

An Et_2O (5 mL) solution of KCp′ (460 mg, 2.61 mmol) was added to a pale-green solution of $U(BH_4)_4$ (250 mg, 0.841 mmol), also dissolved in Et_2O (5 mL). White solids precipitated (presumably KBH_4) as the solution quickly turned orange and then slowly changed to dark red (30 min). After stirring the mixture for an additional 12 h, volatiles were removed under reduced pressure, and the product was extracted into hexane leaving white solids behind (presumably KBH_4). Removal of the volatiles under reduced pressure gave Cp′$_3$U(BH$_4$) (496 mg, 89%) as a dark wine-red solid. X-ray quality crystals were grown from a concentrated ether solution at 253 K.

Table 2
Experimental details.

Crystal data	
Chemical formula	$[U(BH_4)(C_8H_{13}Si)_3]$
M_r	664.69
Crystal system, space group	Triclinic, $P\overline{1}$
Temperature (K)	112
a, *b*, *c* (Å)	8.7530 (15), 12.217 (2), 13.657 (2)
α, β, γ (°)	94.159 (3), 96.016 (3), 103.256 (3)
V (Å^3)	1406.6 (4)
Z	2
Radiation type	Mo $K\alpha$
μ (mm^{-1})	5.91
Crystal size (mm)	0.88 × 0.62 × 0.17
Data collection	
Diffractometer	Bruker D8 Quest with Photon II detector
Absorption correction	Multi-scan (*SADABS*; Krause *et al.*, 2015)
T_{min}, T_{max}	0.413, 0.747
No. of measured, independent and observed [$I > 2\sigma(I)$] reflections	30231, 10686, 9355
R_{int}	0.055
(sin $\theta/\lambda)_{max}$ (Å^{-1})	0.769
Refinement	
$R[F^2 > 2\sigma(F^2)]$, $wR(F^2)$, S	0.037, 0.102, 1.07
No. of reflections	10686
No. of parameters	274
H-atom treatment	H atoms treated by a mixture of independent and constrained refinement
$\Delta\rho_{max}$, $\Delta\rho_{min}$ (e Å^{-3})	3.87, −2.72

Computer programs: *APEX3* and *SAINT* (Bruker, 2018), *SHELXS97* (Sheldrick, 2008), *SHELXL2018/3* (Sheldrick, 2015), and *SHELXTL2018/3* (Sheldrick, 2008).

7. Refinement

Crystal data, data collection and structure refinement details are summarized in Table 2. Analytical scattering factors neutral atoms were used throughout the analysis. A 3-D

rendering of the molecule can be found at the following web address: https://submission.iucr.org/jtkt/serve/z/Utgd9EjfTrqJ-VoXA/zz0000/0/.

C—H bond distances were constrained to 0.95 Å for cyclopentadienyl C—H moieties, and to 0.98 Å for aliphatic CH_3 moieties, respectively. Methyl torsion angles were not refined but constrained to be staggered. The borohydride H atoms were located from a difference-Fourier map and their positions were freely refined. U_{iso}(H) values were set to a multiple of U_{eq}(C/B) with 1.5 for CH_3 and BH_4 and 1.2 for C—H units, respectively.

Acknowledgements

We wish to thank Robert T. Pain (University of New Mexico) for the gift of $U(BH_4)_4$. We also wish to thank Dr Joseph W. Ziller (UC-Irvine) for helpful discussions.

Funding information

Funding for this research was provided by: U.S. Department of Energy, Office of Science, Office of Basic Energy Sciences, Heavy Element Chemistry program (grant No. 2020LANLE372 to SAK, BLS; grant No. DE-SC0004739 to WJE); U.S. Department of Energy, Office of Science, Office of Workforce Development for Teachers and Scientists, Oak Ridge Institute for Science and Education (ORISE), Office of Science Graduate Student Research (SCGSR) program. (contract No. DE-AC05-06OR23100 to CJW); Los Alamos, Director's Postdoctoral Fellowship (award to JNC); U.S. Department of Energy, NNSA, Triad National Security, LLC (contract No. 89233218CNA000001).

References

Arliguie, T., Blug, M., Le Floch, P., Mézailles, N., Thuéry, P. & Ephritikhine, M. (2008). *Organometallics*, **27**, 4158–4165.
Arnold, P. L., Farnaby, J. H., Gardiner, M. G. & Love, J. B. (2015). *Organometallics*, **34**, 2114–2117.
Baudry, D., Bulot, E., Charpin, P., Ephritikhine, M., Lance, M., Nierlich, M. & Vigner, J. (1989). *J. Organomet. Chem.* **371**, 163–174.
Baudry, D., Charpin, P., Ephritikhine, M., Folcher, G., Lambard, J., Lance, M., Nierlich, M. & Vigner, J. (1985). *J. Chem. Soc. Chem. Commun.* pp. 1553–1554.
Baudry, D., Ephritikhine, M., Nief, F., Ricard, L. & Mathey, F. (1990). *Angew. Chem. Int. Ed. Engl.* **29**, 1485–1486.
Bernstein, E. R., Hamilton, W. C., Keiderling, T. A., La Placa, S. J., Lippard, S. J. & Mayerle, J. J. (1972). *Inorg. Chem.* **11**, 3009–3016.
Berthet, J.-C. & Ephritikhine, M. (1992). *New J. Chem.* **16**, 767–768.
Berthet, J.-C., Le Maréchal, J.-F., Nierlich, M., Lance, M., Vigner, J. & Ephritikhine, M. (1991). *J. Organomet. Chem.* **408**, 335–341.
Blake, P. C., Lappert, M. F., Taylor, R. G., Atwood, J. L., Hunter, W. E. & Zhang, H. (1995). *J. Chem. Soc. Dalton Trans.* pp. 3335–3341.
Bruker (2018). *APEX3*, and *SAINT*. Bruker AXS Inc., Madison, Wisconsin, USA.
Cendrowski-Guillaume, S. M., Nierlich, M. & Ephritikhine, M. (2002). *J. Organomet. Chem.* **643–644**, 209–213.
Daly, S. R., Ephritikhine, M. & Girolami, G. S. (2012). *Polyhedron*, **33**, 41–44.
Daly, S. R. & Girolami, G. S. (2010). *Chem. Commun.* **46**, 407–408.
Daly, S. R., Piccoli, P. M., Schultz, A. J., Todorova, T. K., Gagliardi, L. & Girolami, G. S. (2010). *Angew. Chem. Int. Ed.* **49**, 3379–3381.
Elkechai, A., Boucekkine, A., Belkhiri, L., Amarouche, M., Clappe, C., Hauchard, D. & Ephritikhine, M. (2009). *Dalton Trans.* pp. 2843–2849.
Ephritikhine, M. (1997). *Chem. Rev.* **97**, 2193–2242.
Gradoz, P., Baudry, D., Ephritikhine, M., Lance, M., Nierlich, M. & Vigner, J. (1994). *J. Organomet. Chem.* **466**, 107–118.
Groom, C. R., Bruno, I. J., Lightfoot, M. P. & Ward, S. C. (2016). *Acta Cryst.* B**72**, 171–179.
Hoekstra, H. R. & Katz, J. J. (1949). *J. Am. Chem. Soc.* **71**, 2488–2492.
Krause, L., Herbst-Irmer, R., Sheldrick, G. M. & Stalke, D. (2015). *J. Appl. Cryst.* **48**, 3–10.
Liptrot, D. J., Guo, J.-D., Nagase, S. & Power, P. P. (2016). *Angew. Chem. Int. Ed.* **55**, 14766–14769.
MacDonald, M. R., Fieser, M. E., Bates, J. E., Ziller, J. W., Furche, F. & Evans, W. J. (2013). *J. Am. Chem. Soc.* **135**, 13310–13313.
Marsh, R. E., Kapon, M., Hu, S. & Herbstein, F. H. (2002). *Acta Cryst.* B**58**, 62–77.
Mehdoui, T., Berthet, J.-C., Thuéry, P. & Ephritikhine, M. (2004). *Eur. J. Inorg. Chem.* pp. 1996–2000.
Peterson, J. K., MacDonald, M. R., Ziller, J. W. & Evans, W. J. (2013). *Organometallics*, **32**, 2625–2631.
Réant, B. L. L., Berryman, V. E. J., Seed, J. A., Basford, A. R., Formanuik, A., Wooles, A. J., Kaltsoyannis, N., Liddle, S. T. & Mills, D. P. (2020). *Chem. Commun.* **56**, 12620–12623.
Rebizant, J., Spirlet, M. R., Bettonville, S. & Goffart, J. (1989). *Acta Cryst.* C**45**, 1509–1511.
Ryan, R. R., Salazar, K. V., Sauer, N. N. & Ritchey, J. M. (1989). *Inorg. Chim. Acta*, **162**, 221–225.
Schlesinger, H. I. & Brown, H. C. (1953). *J. Am. Chem. Soc.* **75**, 219–221.
Schock, L. E., Seyam, A. M., Sabat, M. & Marks, T. J. (1988). *Polyhedron*, **7**, 1517–1529.
Sheldrick, G. M. (2008). *Acta Cryst.* A**64**, 112–122.
Sheldrick, G. M. (2015). *Acta Cryst.* C**71**, 3–8.
Tsoureas, N. & Cloke, F. G. N. (2018). *Chem. Commun.* **54**, 8830–8833.
Wedal, J. C., Bekoe, S., Ziller, J. W., Furche, F. & Evans, W. J. (2019). *Dalton Trans.* **48**, 16633–16640.
Windorff, C. J. & Evans, W. J. (2014). *Organometallics*, **33**, 3786–3791.
Windorff, C. J., MacDonald, M. R., Ziller, J. W. & Evans, W. J. (2017). *Z. Anorg. Allg. Chem.* **643**, 2011–2018.
Zanella, P., Brianese, N., Casellato, U., Ossola, F., Porchia, M., Rossetto, G. & Graziani, R. (1988). *Inorg. Chim. Acta*, **144**, 129–134.
Zanella, P., De Paoli, G., Bombieri, G., Zanotti, G. & Rossi, R. (1977). *J. Organomet. Chem.* **142**, C21–C24.

supporting information

Acta Cryst. (2021). E**77**, 383-389 [https://doi.org/10.1107/S2056989021002425]

Crystallographic characterization of $(C_5H_4SiMe_3)_3U(BH_4)$

Cory J. Windorff, Justin N. Cross, Brian L. Scott, Stosh A. Kozimor and William J. Evans

Computing details

Data collection: *APEX3* (Bruker, 2018); cell refinement: *APEX3* (Bruker, 2018); data reduction: *SAINT* (Bruker, 2018); program(s) used to solve structure: *SHELXS97* (Sheldrick, 2008); program(s) used to refine structure: *SHELXL2018/3* (Sheldrick, 2015); molecular graphics: *SHELXTL2018/3* (Sheldrick, 2008); software used to prepare material for publication: *SHELXTL2018/3* (Sheldrick, 2008).

(Borohydrido-κ^3H)tris[η^5-(trimethylsilyl)cyclopentadienyl]uranium(IV)

Crystal data

$[U(BH_4)(C_8H_{13}Si)_3]$
M_r = 664.69
Triclinic, $P\overline{1}$
a = 8.7530 (15) Å
b = 12.217 (2) Å
c = 13.657 (2) Å
α = 94.159 (3)°
β = 96.016 (3)°
γ = 103.256 (3)°
V = 1406.6 (4) Å^3
Z = 2
$F(000)$ = 652
D_x = 1.569 Mg m^{-3}
Mo $K\alpha$ radiation, λ = 0.71073 Å
Cell parameters from 30231 reflections
θ = 2.4–33.1°
μ = 5.91 mm^{-1}
T = 112 K
Plate, red
0.88 × 0.62 × 0.17 mm

Data collection

Bruker D8 Quest with Photon II detector diffractometer
Radiation source: IμS 3.0 microfocus
ω scans
Absorption correction: multi-scan (SADABS; Krause *et al.*, 2015)
T_{min} = 0.413, T_{max} = 0.747
30231 measured reflections
10686 independent reflections
9355 reflections with $I > 2\sigma(I)$
R_{int} = 0.055
θ_{max} = 33.1°, θ_{min} = 2.4°
h = −13→13
k = −18→18
l = −20→20

Refinement

Refinement on F^2
Least-squares matrix: full
$R[F^2 > 2\sigma(F^2)]$ = 0.037
$wR(F^2)$ = 0.102
S = 1.07
10686 reflections
274 parameters
0 restraints
Primary atom site location: structure-invariant direct methods
Secondary atom site location: difference Fourier map
Hydrogen site location: mixed
H atoms treated by a mixture of independent and constrained refinement
$w = 1/[\sigma^2(F_o^2) + (0.0549P)^2]$ where $P = (F_o^2 + 2F_c^2)/3$
$(\Delta/\sigma)_{max}$ = 0.002
$\Delta\rho_{max}$ = 3.87 e Å^{-3}
$\Delta\rho_{min}$ = −2.72 e Å^{-3}

Special details

Geometry. All esds (except the esd in the dihedral angle between two l.s. planes) are estimated using the full covariance matrix. The cell esds are taken into account individually in the estimation of esds in distances, angles and torsion angles; correlations between esds in cell parameters are only used when they are defined by crystal symmetry. An approximate (isotropic) treatment of cell esds is used for estimating esds involving l.s. planes.

Fractional atomic coordinates and isotropic or equivalent isotropic displacement parameters (Å²)

	x	*y*	*z*	U_{iso}*/U_{eq}
U1	0.51249 (2)	0.16808 (2)	0.26353 (2)	0.00963 (4)
B1	0.8150 (5)	0.2329 (4)	0.3009 (4)	0.0177 (8)
H1A	0.761 (6)	0.294 (5)	0.308 (4)	0.027*
H1B	0.771 (6)	0.205 (5)	0.219 (4)	0.027*
H1C	0.762 (6)	0.166 (5)	0.348 (4)	0.027*
H1D	0.944 (6)	0.271 (5)	0.317 (4)	0.027*
Si1	0.76504 (13)	0.39347 (9)	0.07862 (8)	0.0156 (2)
Si2	0.71528 (13)	0.35432 (9)	0.54090 (9)	0.0161 (2)
Si3	0.79753 (13)	−0.07373 (10)	0.23562 (8)	0.0161 (2)
C1	0.5747 (4)	0.3269 (3)	0.1255 (3)	0.0134 (6)
C2	0.4548 (4)	0.2353 (3)	0.0762 (3)	0.0142 (7)
H2	0.467664	0.185642	0.022485	0.017*
C3	0.3126 (4)	0.2291 (3)	0.1192 (3)	0.0168 (7)
H3A	0.205686	0.182752	0.090235	0.020*
C4	0.3423 (5)	0.3169 (3)	0.1952 (3)	0.0194 (8)
H4A	0.259820	0.343109	0.229549	0.023*
C5	0.5036 (5)	0.3754 (3)	0.2021 (3)	0.0170 (7)
H5A	0.551554	0.449334	0.242324	0.020*
C6	0.8516 (6)	0.2832 (4)	0.0182 (4)	0.0258 (9)
H6A	0.773894	0.237713	−0.034755	0.039*
H6B	0.946750	0.320007	−0.009698	0.039*
H6C	0.879493	0.234315	0.067481	0.039*
C7	0.9080 (5)	0.4833 (4)	0.1805 (4)	0.0259 (9)
H7A	0.935861	0.435704	0.231009	0.039*
H7B	1.003659	0.521095	0.153741	0.039*
H7C	0.859331	0.540147	0.210342	0.039*
C8	0.7126 (6)	0.4851 (4)	−0.0173 (4)	0.0284 (10)
H8A	0.637627	0.438442	−0.070950	0.043*
H8B	0.664218	0.541988	0.012768	0.043*
H8C	0.808545	0.522937	−0.043833	0.043*
C9	0.5445 (4)	0.2558 (3)	0.4617 (3)	0.0139 (6)
C10	0.5031 (4)	0.1358 (3)	0.4589 (3)	0.0129 (6)
H10A	0.566960	0.090586	0.496241	0.016*
C11	0.3457 (4)	0.0938 (3)	0.4159 (3)	0.0148 (7)
H11A	0.280490	0.015468	0.418243	0.018*
C12	0.2877 (4)	0.1864 (3)	0.3859 (3)	0.0159 (7)
H12A	0.174487	0.184244	0.363546	0.019*
C13	0.4089 (5)	0.2856 (3)	0.4155 (3)	0.0156 (7)
H13	0.400650	0.360371	0.406008	0.019*

C14	0.7834 (5)	0.4881 (3)	0.4818 (4)	0.0236 (9)
H14A	0.694252	0.523095	0.467930	0.035*
H14B	0.867433	0.540488	0.526781	0.035*
H14C	0.823995	0.470669	0.419794	0.035*
C15	0.6386 (6)	0.3890 (4)	0.6594 (3)	0.0269 (9)
H15A	0.553651	0.428013	0.645944	0.040*
H15B	0.597529	0.319142	0.688904	0.040*
H15C	0.724665	0.438154	0.705407	0.040*
C16	0.8764 (5)	0.2804 (4)	0.5706 (3)	0.0226 (8)
H16A	0.965381	0.332556	0.612059	0.034*
H16B	0.836522	0.215057	0.606193	0.034*
H16C	0.911947	0.254911	0.509097	0.034*
C17	0.6012 (4)	−0.0360 (3)	0.2171 (3)	0.0128 (6)
C18	0.4764 (5)	−0.0648 (3)	0.2755 (3)	0.0140 (6)
H18	0.485999	−0.088223	0.340226	0.017*
C19	0.3343 (4)	−0.0530 (3)	0.2215 (3)	0.0153 (7)
H19	0.232617	−0.068713	0.243279	0.018*
C20	0.3699 (4)	−0.0141 (3)	0.1306 (3)	0.0145 (7)
H20A	0.290811	−0.013775	0.072251	0.017*
C21	0.5350 (4)	−0.0017 (3)	0.1283 (3)	0.0130 (6)
H21A	0.589324	0.009939	0.067662	0.016*
C22	0.8854 (5)	−0.0487 (4)	0.3683 (3)	0.0238 (9)
H22A	0.904791	0.031903	0.390761	0.036*
H22B	0.811913	−0.092648	0.408388	0.036*
H22C	0.985486	−0.072076	0.375288	0.036*
C23	0.7622 (7)	−0.2283 (4)	0.1955 (4)	0.0334 (11)
H23A	0.716059	−0.243268	0.125928	0.050*
H23B	0.862889	−0.250933	0.203265	0.050*
H23C	0.689316	−0.271505	0.236365	0.050*
C24	0.9339 (5)	0.0070 (4)	0.1537 (4)	0.0277 (10)
H24A	0.883975	−0.008159	0.084891	0.042*
H24B	0.954902	0.088142	0.174393	0.042*
H24C	1.033665	−0.016878	0.159288	0.042*

Atomic displacement parameters (Å²)

	U^{11}	U^{22}	U^{33}	U^{12}	U^{13}	U^{23}
U1	0.00980 (6)	0.01025 (6)	0.00983 (7)	0.00336 (4)	0.00194 (4)	0.00341 (4)
B1	0.0131 (18)	0.019 (2)	0.021 (2)	0.0041 (15)	0.0016 (16)	0.0059 (16)
Si1	0.0167 (5)	0.0131 (4)	0.0176 (5)	0.0025 (4)	0.0052 (4)	0.0052 (4)
Si2	0.0188 (5)	0.0123 (4)	0.0163 (5)	0.0030 (4)	0.0004 (4)	0.0002 (4)
Si3	0.0160 (5)	0.0195 (5)	0.0161 (5)	0.0099 (4)	0.0025 (4)	0.0049 (4)
C1	0.0143 (15)	0.0126 (15)	0.0135 (16)	0.0032 (12)	0.0010 (12)	0.0050 (12)
C2	0.0163 (16)	0.0158 (16)	0.0109 (16)	0.0038 (13)	0.0015 (13)	0.0037 (12)
C3	0.0140 (16)	0.0207 (18)	0.0172 (18)	0.0051 (13)	0.0010 (13)	0.0098 (14)
C4	0.0163 (17)	0.0192 (18)	0.028 (2)	0.0106 (14)	0.0061 (15)	0.0141 (16)
C5	0.0186 (17)	0.0148 (16)	0.0210 (19)	0.0079 (13)	0.0051 (14)	0.0091 (14)
C6	0.030 (2)	0.020 (2)	0.029 (2)	0.0048 (17)	0.0154 (19)	0.0026 (17)

C7	0.024 (2)	0.021 (2)	0.030 (2)	−0.0006 (16)	0.0056 (18)	0.0030 (17)
C8	0.028 (2)	0.029 (2)	0.032 (3)	0.0063 (18)	0.0100 (19)	0.021 (2)
C9	0.0145 (15)	0.0117 (15)	0.0165 (17)	0.0045 (12)	0.0024 (13)	0.0022 (12)
C10	0.0168 (16)	0.0122 (15)	0.0102 (15)	0.0033 (12)	0.0028 (12)	0.0028 (12)
C11	0.0148 (15)	0.0169 (16)	0.0132 (16)	0.0016 (13)	0.0061 (13)	0.0057 (13)
C12	0.0119 (15)	0.0236 (18)	0.0143 (17)	0.0067 (13)	0.0046 (13)	0.0026 (14)
C13	0.0167 (16)	0.0175 (17)	0.0145 (17)	0.0076 (13)	0.0025 (13)	0.0023 (13)
C14	0.026 (2)	0.0122 (17)	0.032 (2)	0.0031 (15)	0.0054 (18)	0.0032 (16)
C15	0.037 (2)	0.023 (2)	0.018 (2)	0.0031 (18)	0.0037 (18)	−0.0048 (16)
C16	0.0228 (19)	0.0204 (19)	0.025 (2)	0.0080 (15)	−0.0036 (16)	0.0027 (16)
C17	0.0141 (15)	0.0125 (15)	0.0126 (16)	0.0041 (12)	0.0025 (12)	0.0029 (12)
C18	0.0190 (17)	0.0126 (15)	0.0104 (16)	0.0033 (13)	0.0025 (13)	0.0024 (12)
C19	0.0137 (15)	0.0127 (15)	0.0182 (18)	−0.0003 (12)	0.0032 (13)	0.0031 (13)
C20	0.0140 (15)	0.0176 (16)	0.0097 (16)	0.0018 (13)	−0.0030 (12)	−0.0001 (12)
C21	0.0149 (16)	0.0140 (15)	0.0111 (16)	0.0063 (12)	0.0007 (12)	−0.0007 (12)
C22	0.0220 (19)	0.033 (2)	0.020 (2)	0.0142 (17)	0.0007 (16)	0.0059 (17)
C23	0.040 (3)	0.025 (2)	0.041 (3)	0.022 (2)	0.001 (2)	−0.001 (2)
C24	0.023 (2)	0.038 (3)	0.030 (2)	0.0164 (19)	0.0102 (18)	0.014 (2)

Geometric parameters (Å, º)

U1—B1	2.568 (4)	C7—H7B	0.9800
U1—C21	2.731 (4)	C7—H7C	0.9800
U1—C10	2.732 (4)	C8—H8A	0.9800
U1—C20	2.733 (4)	C8—H8B	0.9800
U1—C5	2.740 (4)	C8—H8C	0.9800
U1—C12	2.748 (4)	C9—C13	1.419 (5)
U1—C11	2.754 (3)	C9—C10	1.424 (5)
U1—C4	2.755 (4)	C10—C11	1.403 (5)
U1—C3	2.755 (4)	C10—H10A	1.0000
U1—H1A	2.35 (5)	C11—C12	1.411 (5)
U1—H1B	2.35 (5)	C11—H11A	1.0000
U1—H1C	2.36 (5)	C12—C13	1.417 (5)
B1—H1A	0.98 (6)	C12—H12A	1.0000
B1—H1B	1.15 (6)	C13—H13	0.9500
B1—H1C	1.12 (5)	C14—H14A	0.9800
B1—H1D	1.11 (5)	C14—H14B	0.9800
Si1—C7	1.868 (5)	C14—H14C	0.9800
Si1—C8	1.871 (4)	C15—H15A	0.9800
Si1—C6	1.872 (5)	C15—H15B	0.9800
Si1—C1	1.877 (4)	C15—H15C	0.9800
Si2—C16	1.867 (4)	C16—H16A	0.9800
Si2—C9	1.871 (4)	C16—H16B	0.9800
Si2—C15	1.873 (5)	C16—H16C	0.9800
Si2—C14	1.877 (4)	C17—C18	1.415 (5)
Si3—C22	1.867 (5)	C17—C21	1.421 (5)
Si3—C23	1.873 (5)	C18—C19	1.420 (5)
Si3—C17	1.876 (4)	C18—H18	0.9500

Si3—C24	1.884 (5)	C19—C20	1.402 (5)
C1—C2	1.418 (5)	C19—H19	0.9500
C1—C5	1.432 (6)	C20—C21	1.421 (5)
C2—C3	1.420 (5)	C20—H20A	1.0000
C2—H2	0.9500	C21—H21A	1.0000
C3—C4	1.396 (6)	C22—H22A	0.9800
C3—H3A	1.0000	C22—H22B	0.9800
C4—C5	1.418 (5)	C22—H22C	0.9800
C4—H4A	1.0000	C23—H23A	0.9800
C5—H5A	1.0000	C23—H23B	0.9800
C6—H6A	0.9800	C23—H23C	0.9800
C6—H6B	0.9800	C24—H24A	0.9800
C6—H6C	0.9800	C24—H24B	0.9800
C7—H7A	0.9800	C24—H24C	0.9800

B1—U1—C21	91.29 (14)	C3—C4—H4A	125.3
B1—U1—C10	88.27 (13)	C5—C4—H4A	125.3
C21—U1—C10	121.25 (11)	U1—C4—H4A	125.3
B1—U1—C20	121.42 (14)	C4—C5—C1	108.8 (4)
C21—U1—C20	30.15 (11)	C4—C5—U1	75.7 (2)
C10—U1—C20	116.28 (11)	C1—C5—U1	77.6 (2)
B1—U1—C5	89.68 (13)	C4—C5—H5A	124.8
C21—U1—C5	119.23 (12)	C1—C5—H5A	124.8
C10—U1—C5	119.52 (12)	U1—C5—H5A	124.8
C20—U1—C5	115.78 (12)	Si1—C6—H6A	109.5
B1—U1—C12	128.78 (14)	Si1—C6—H6B	109.5
C21—U1—C12	131.96 (12)	H6A—C6—H6B	109.5
C10—U1—C12	48.97 (11)	Si1—C6—H6C	109.5
C20—U1—C12	104.45 (12)	H6A—C6—H6C	109.5
C5—U1—C12	89.90 (12)	H6B—C6—H6C	109.5
B1—U1—C11	117.73 (13)	Si1—C7—H7A	109.5
C21—U1—C11	113.80 (11)	Si1—C7—H7B	109.5
C10—U1—C11	29.63 (11)	H7A—C7—H7B	109.5
C20—U1—C11	95.57 (11)	Si1—C7—H7C	109.5
C5—U1—C11	118.89 (12)	H7A—C7—H7C	109.5
C12—U1—C11	29.73 (11)	H7B—C7—H7C	109.5
B1—U1—C4	119.54 (13)	Si1—C8—H8A	109.5
C21—U1—C4	115.96 (13)	Si1—C8—H8B	109.5
C10—U1—C4	114.79 (12)	H8A—C8—H8B	109.5
C20—U1—C4	98.00 (13)	Si1—C8—H8C	109.5
C5—U1—C4	29.91 (11)	H8A—C8—H8C	109.5
C12—U1—C4	70.43 (12)	H8B—C8—H8C	109.5
C11—U1—C4	99.66 (12)	C13—C9—C10	105.6 (3)
B1—U1—C3	129.05 (13)	C13—C9—Si2	125.9 (3)
C21—U1—C3	87.02 (12)	C10—C9—Si2	126.4 (3)
C10—U1—C3	134.56 (12)	C11—C10—C9	109.8 (3)
C20—U1—C3	69.70 (12)	C11—C10—U1	76.0 (2)
C5—U1—C3	49.08 (12)	C9—C10—U1	77.7 (2)

C12—U1—C3	85.59 (12)	C11—C10—H10A	124.4
C11—U1—C3	109.24 (11)	C9—C10—H10A	124.4
C4—U1—C3	29.34 (13)	U1—C10—H10A	124.4
B1—U1—H1A	22.4 (14)	C10—C11—C12	107.6 (3)
C21—U1—H1A	110.3 (14)	C10—C11—U1	74.3 (2)
C10—U1—H1A	88.4 (14)	C12—C11—U1	74.9 (2)
C20—U1—H1A	139.8 (14)	C10—C11—H11A	125.7
C5—U1—H1A	70.3 (13)	C12—C11—H11A	125.7
C12—U1—H1A	115.5 (14)	U1—C11—H11A	125.7
C11—U1—H1A	116.7 (14)	C11—C12—C13	107.6 (3)
C4—U1—H1A	99.3 (13)	C11—C12—U1	75.4 (2)
C3—U1—H1A	116.2 (13)	C13—C12—U1	76.6 (2)
B1—U1—H1B	26.5 (14)	C11—C12—H12A	125.4
C21—U1—H1B	70.8 (14)	C13—C12—H12A	125.4
C10—U1—H1B	113.0 (14)	U1—C12—H12A	125.4
C20—U1—H1B	100.0 (14)	C12—C13—C9	109.4 (3)
C5—U1—H1B	85.6 (13)	C12—C13—H13	125.3
C12—U1—H1B	154.6 (14)	C9—C13—H13	125.3
C11—U1—H1B	141.1 (13)	Si2—C14—H14A	109.5
C4—U1—H1B	113.1 (13)	Si2—C14—H14B	109.5
C3—U1—H1B	109.6 (13)	H14A—C14—H14B	109.5
H1A—U1—H1B	39.9 (19)	Si2—C14—H14C	109.5
B1—U1—H1C	25.8 (13)	H14A—C14—H14C	109.5
C21—U1—H1C	90.4 (14)	H14B—C14—H14C	109.5
C10—U1—H1C	66.9 (14)	Si2—C15—H15A	109.5
C20—U1—H1C	116.7 (13)	Si2—C15—H15B	109.5
C5—U1—H1C	112.4 (13)	H15A—C15—H15B	109.5
C12—U1—H1C	114.2 (14)	Si2—C15—H15C	109.5
C11—U1—H1C	94.8 (13)	H15A—C15—H15C	109.5
C4—U1—H1C	140.7 (13)	H15B—C15—H15C	109.5
C3—U1—H1C	154.7 (13)	Si2—C16—H16A	109.5
H1A—U1—H1C	42.1 (18)	Si2—C16—H16B	109.5
H1B—U1—H1C	46.4 (18)	H16A—C16—H16B	109.5
U1—B1—H1A	66 (3)	Si2—C16—H16C	109.5
U1—B1—H1B	66 (3)	H16A—C16—H16C	109.5
H1A—B1—H1B	97 (4)	H16B—C16—H16C	109.5
U1—B1—H1C	67 (3)	C18—C17—C21	106.5 (3)
H1A—B1—H1C	107 (4)	C18—C17—Si3	126.3 (3)
H1B—B1—H1C	110 (4)	C21—C17—Si3	125.2 (3)
U1—B1—H1D	174 (3)	C17—C18—C19	108.8 (3)
H1A—B1—H1D	108 (4)	C17—C18—H18	125.6
H1B—B1—H1D	115 (4)	C19—C18—H18	125.6
H1C—B1—H1D	118 (4)	C20—C19—C18	108.2 (3)
C7—Si1—C8	109.1 (2)	C20—C19—H19	125.9
C7—Si1—C6	111.5 (2)	C18—C19—H19	125.9
C8—Si1—C6	108.4 (2)	C19—C20—C21	107.5 (3)
C7—Si1—C1	110.74 (19)	C19—C20—U1	77.0 (2)
C8—Si1—C1	106.02 (19)	C21—C20—U1	74.8 (2)

C6—Si1—C1	110.83 (18)	C19—C20—H20A	125.5
C16—Si2—C9	109.96 (19)	C21—C20—H20A	125.5
C16—Si2—C15	107.7 (2)	U1—C20—H20A	125.5
C9—Si2—C15	105.7 (2)	C20—C21—C17	109.0 (3)
C16—Si2—C14	113.1 (2)	C20—C21—U1	75.0 (2)
C9—Si2—C14	111.05 (19)	C17—C21—U1	78.9 (2)
C15—Si2—C14	109.0 (2)	C20—C21—H21A	124.6
C22—Si3—C23	108.2 (2)	C17—C21—H21A	124.6
C22—Si3—C17	111.93 (19)	U1—C21—H21A	124.6
C23—Si3—C17	107.1 (2)	Si3—C22—H22A	109.5
C22—Si3—C24	111.8 (2)	Si3—C22—H22B	109.5
C23—Si3—C24	108.4 (3)	H22A—C22—H22B	109.5
C17—Si3—C24	109.23 (18)	Si3—C22—H22C	109.5
C2—C1—C5	105.6 (3)	H22A—C22—H22C	109.5
C2—C1—Si1	126.1 (3)	H22B—C22—H22C	109.5
C5—C1—Si1	126.4 (3)	Si3—C23—H23A	109.5
C1—C2—C3	109.7 (4)	Si3—C23—H23B	109.5
C1—C2—H2	125.2	H23A—C23—H23B	109.5
C3—C2—H2	125.2	Si3—C23—H23C	109.5
C4—C3—C2	107.5 (3)	H23A—C23—H23C	109.5
C4—C3—U1	75.3 (2)	H23B—C23—H23C	109.5
C2—C3—U1	75.9 (2)	Si3—C24—H24A	109.5
C4—C3—H3A	125.5	Si3—C24—H24B	109.5
C2—C3—H3A	125.5	H24A—C24—H24B	109.5
U1—C3—H3A	125.5	Si3—C24—H24C	109.5
C3—C4—C5	108.4 (4)	H24A—C24—H24C	109.5
C3—C4—U1	75.3 (2)	H24B—C24—H24C	109.5
C5—C4—U1	74.4 (2)		

C7—Si1—C1—C2	−164.8 (3)	Si2—C9—C10—U1	−128.1 (3)
C8—Si1—C1—C2	76.9 (4)	C9—C10—C11—C12	3.1 (4)
C6—Si1—C1—C2	−40.5 (4)	U1—C10—C11—C12	−68.1 (3)
C7—Si1—C1—C5	33.1 (4)	C9—C10—C11—U1	71.2 (3)
C8—Si1—C1—C5	−85.2 (4)	C10—C11—C12—C13	−2.8 (4)
C6—Si1—C1—C5	157.4 (3)	U1—C11—C12—C13	−70.5 (3)
C5—C1—C2—C3	1.5 (4)	C10—C11—C12—U1	67.7 (3)
Si1—C1—C2—C3	−163.6 (3)	C11—C12—C13—C9	1.6 (4)
C1—C2—C3—C4	0.3 (4)	U1—C12—C13—C9	−68.1 (3)
C1—C2—C3—U1	−69.1 (3)	C10—C9—C13—C12	0.3 (4)
C2—C3—C4—C5	−2.0 (4)	Si2—C9—C13—C12	−163.7 (3)
U1—C3—C4—C5	67.7 (3)	C22—Si3—C17—C18	−45.2 (4)
C2—C3—C4—U1	−69.7 (3)	C23—Si3—C17—C18	73.3 (4)
C3—C4—C5—C1	3.0 (4)	C24—Si3—C17—C18	−169.5 (4)
U1—C4—C5—C1	71.3 (3)	C22—Si3—C17—C21	153.2 (3)
C3—C4—C5—U1	−68.3 (3)	C23—Si3—C17—C21	−88.3 (4)
C2—C1—C5—C4	−2.8 (4)	C24—Si3—C17—C21	28.9 (4)
Si1—C1—C5—C4	162.3 (3)	C21—C17—C18—C19	2.5 (4)
C2—C1—C5—U1	67.2 (2)	Si3—C17—C18—C19	−161.9 (3)

Si1—C1—C5—U1	−127.7 (3)	C17—C18—C19—C20	−1.5 (4)
C16—Si2—C9—C13	−172.4 (3)	C18—C19—C20—C21	0.0 (4)
C15—Si2—C9—C13	71.6 (4)	C18—C19—C20—U1	−69.3 (3)
C14—Si2—C9—C13	−46.5 (4)	C19—C20—C21—C17	1.6 (4)
C16—Si2—C9—C10	26.8 (4)	U1—C20—C21—C17	72.3 (3)
C15—Si2—C9—C10	−89.2 (4)	C19—C20—C21—U1	−70.8 (3)
C14—Si2—C9—C10	152.7 (3)	C18—C17—C21—C20	−2.5 (4)
C13—C9—C10—C11	−2.1 (4)	Si3—C17—C21—C20	162.1 (3)
Si2—C9—C10—C11	161.8 (3)	C18—C17—C21—U1	67.2 (3)
C13—C9—C10—U1	68.0 (3)	Si3—C17—C21—U1	−128.1 (3)